

COMPACT FEL-DRIVEN INVERSE COMPTON SCATTERING GAMMA-RAY SOURCE

M. Placidi¹, G. Penn, Lawrence Berkeley National Laboratory, Berkeley, CA 94720, USA
S. Di Mitri[†], Elettra - Sincrotrone Trieste S.C.p.A., 34149 Basovizza, Trieste, Italy
C. Pellegrini², Stanford Linear Accelerator Center, Menlo Park, CA 94025, USA

¹on leave

²also at University of California, Los Angeles, CA 90095, USA

Abstract

We explore the feasibility of a compact source of quasi-monochromatic, multi-MeV gamma-rays based on Inverse Compton Scattering (ICS) from a high intensity ultra-violet (UV) beam generated in a free-electron laser by the electron beam itself [1]. This scheme introduces a stronger relationship between the energy of the scattered photons and that of the electron beam, resulting in a device much more compact than a classic ICS for a given scattered energy. The same electron beam is used to produce gamma-rays in the 10-20 MeV range and UV radiation in the 10-15 eV range, in a $\sim 4 \times 22$ m² footprint system.

INTRODUCTION

We discuss the feasibility and the performance of an Inverse Compton Scattering (ICS)-based scheme where the electron beam interacts with its own radiation emitted in a Free Electron Laser (FEL). The energy of the outgoing radiation has a steeper dependence on the electron energy than a classical ICS scheme, thus providing a relatively compact layout.

Methods of X-ray production presently include ICS facilities and synchrotron radiation sources from insertion devices in electron storage rings. Contrast imaging of massive sculptures would profit [2] from radiation sources more powerful than the X-ray CT industrial instruments operating in the 450 keV range. Specific case studies can be identified, for example, on the basis of the energy content of the scattered light. At low photon energy (up to few MeV), contrast imaging of massive objects in Geo-archeology [2] would greatly benefit from such an intense and compact source, and this was actually the driving case of this work. At photon energies in the 1–10 MeV range, photons propagating through dense materials prompt nuclear reactions, generating *e.g.* alpha particles and neutrons, which can be easily identified and used for isotope separation [3]. At photon energies higher than 10 MeV, the proposed scheme would approach the specifications for an elastic photon-photon scattering source for frontier experiments in QED [4]. As a by-product of the proposed scheme, a naturally synchronized UV beam with large fraction of coherent photons at 100 fs duration level, ideal for pump-probe experiments, would be provided by the FEL. High-flux multi-MeV gamma-ray beams and UV radiation can be simultaneously available for applications in Nuclear Physics, Security Inspections, Cultural

Heritage and UV Science.

FEL-ICS CONCEPT

In a classical ICS process a relativistic electron transfers a fraction of its energy to an incoming laser photon which is scattered in the electron direction of flight with a Doppler-upshifted frequency. The scattered radiation energy

$$E_s = \frac{a_c}{1+X} \gamma^2 \hbar \omega_{ph} \quad (1)$$

exhibits a quadratic energy dependence on the electron energy as the incoming photon energy is constant. The kinematic factor

$$a_c \approx \frac{2(1+\cos\varphi)}{1+(\gamma\theta)^2} \leq 4 \quad (2)$$

modulates the scattered energy via the collision angle φ within the semi-aperture θ of the emission cone, while the term

$$X = 4\gamma \frac{\hbar \omega_{ph}}{m_e} \quad (3)$$

accounts for the recoil of the electron [5].

The FEL-ICS scheme introduces a stronger γ -dependence by making the relativistic electron beam interact with its own UV radiation produced in an FEL [6]. The on-axis FEL radiation wavelength is related to the axial electron velocity β_z and the undulator period λ_u as [7]:

$$\lambda_r = \lambda_u \frac{1-\beta_z}{\beta_z} \approx \frac{\lambda_u}{2\gamma^2} (1 + a_u^2) \quad (4)$$

Here $a_u = K_u = eB_0\lambda_u/2\pi m_e c = 93.4 B_0[T] \lambda_u[m]$ is the helical undulator parameter, B_0 the undulator central magnetic field, e the electron charge. The energy of the FEL photons in terms of the electron energy reads:

$$E_r \equiv \frac{hc}{\lambda_r} = a_{FEL} hc \frac{\gamma^2}{\lambda_u} \quad (5)$$

where we define $a_{FEL} = 2/(1 + a_u^2)$ for on axis undulator radiation. When the FEL photon energy (5) replaces that from the laser in (1), the scattered photon energy can be written as:

$$E_s = a_c E_r \gamma^2 = a_c a_{FEL} hc \frac{\gamma^4}{\lambda_u} \quad (1')$$

The term (3), of the order of 10^{-2} , has been neglected in this kinematic scaling. Introducing the Compton wavelength $\lambda_c = hc/m_e c^2 = 2.426 \times 10^{-3}$ nm, the scattering efficiency, *i.e.* the fraction of the electron energy transferred to the scattered photons, reads

[†] simone.dimitri@elettra.eu

$$\eta \equiv \frac{E_s}{E} = a_c a_{FEL} \frac{\lambda_c}{\lambda_u} \gamma^3 \quad (6)$$

The cubic energy dependence of the scattering efficiency (6) provides compactness to the system, as lower electron energy is required to produce a given upshifted radiation. The UV and the FEL-ICS radiation energies are tunable via the undulator parameter K_u , typically ranging from 1 to 5 in an out-of-vacuum APPLE-II type device [8] or Delta undulator [9].

A conservative figure $\varphi = 25^\circ$ has been assumed for interaction angle resulting from the optimization of different competing requirements, like the scattering efficiency, via the impact parameter a_c , the ICS luminosity and the loop in Fig. 1. The dependence of the incoming (5) and scattered photon energy ($1'$) on the electron beam energy is shown in Fig. 2. It can be gathered that:

- i. The ~ 16 MeV outgoing radiation energy for the 300 MeV electron energy considered in the present study compares with the ~ 3 MeV obtainable in the classical ICS case.
- ii. The scattering efficiencies E_s/E are larger than in the ICS case by one order of magnitude or more in the present energy range, and the comparison dramatically improves with the electron energy.

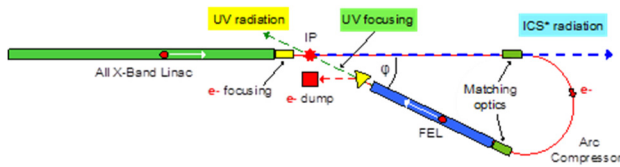


Figure 1: Sketch, not to scale, of the FEL-ICS scheme.

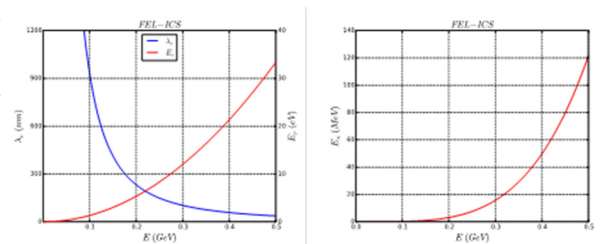


Figure 2: Wavelength of the incoming radiation from undulator with $\lambda_u=20$ mm (left), and scattered radiation energy (right).

FEL-ICS LAYOUT

Facility Footprint

A single-pass conceptual layout of the FEL-ICS scheme is shown in Fig. 1. The main characteristics of the system are summarized in Table 1 and discussed in the following. Trains of electron bunches are produced in an X-Band Linac at 1 kHz repetition rate. A return arc acting as a bunch length compressor [10,11] rises the bunches peak current from 35 A to 500 A and guides them into an FEL undulator operating in the high-gain SASE regime [7,12], long enough to reach saturation. The emerging UV radiation produced by the leading bunches in the train is focused at the IP, where high-energy gamma-rays are produced via Compton interaction with the trailing bunches.

The low value of the Thomson cross section preserves the electron bunch quality for the FEL performance and allows a simultaneous use of the UV radiation for additional applications. The 180° original arc deflection [10] is extended to 205° to comply with the 25° design interaction angle.

The large FEL power compensates for the low Thomson cross-section. The electron bunches and UV radiation are focused to similar transverse spot sizes at the IP to optimize the scattered flux. The electron focusing, bunch compression, and UV optics are all crucial for providing the desired compactness and gamma-ray flux. The short undulator length allowed by bunch compression; an arc compressor length of about 6.5 m and the associated matching optics leave about 2 m for the UV focusing drift downstream the undulator.

Linac and ICS Repetition Rate

We consider a room temperature operation in the original spirit of keeping the photon source within cost-effective limits. Compactness requirements suggest the adoption of high-gradient X-Band technology [13], both for the photo-injector and the accelerating structure. Power dissipation issues associated to the acceleration of electron beams with kHz time structures can be mitigated by choosing operating frequencies in the 11.4–12.0 GHz range in order to increase the RF power transfer efficiency with a higher specific shunt impedance of the structure, proportional to its frequency [14]. Warm X-Band RF technology operating at the above-mentioned repetition rates with a 35 MV/m gradient [15], considerably lower than the 100 MV/m reached at the CTF [16] in laboratory operating conditions, is adopted in this design.

An X-Band photo-injector has been built and commissioned at the X-Band Test Area (XTA) at SLAC with good beam quality. Complementing this injector with a 9 m long, 35 MV/m X-Band accelerating structure sets up an “all X-Band Linac” [17] capable of delivering a 300 MeV electron beam within a ~ 10 m total length. The 1 kHz repetition rate of the ~ 1 μ s long RF pulse containing 100 electron bunches gives an average beam current of about 30 μ A and a 9 kW beam power to the dump. Operation of the X-band linac at the high gradient of 100 MV/m can only be envisioned at a repetition rate lower than 100 Hz, and in single pulse mode. This scenario would therefore shrink the linac length to approximately 3 m for a final beam energy of 300 MeV. However, the average electron beam current, as well as the average FEL-ICS photon flux would be lowered by a factor 1000 with respect to the low-gradient, high pulse rate option, which therefore remains our basic design.

Return Arc Compressor

The bunch final peak current of 0.5 kA is important to obtain a high average FEL photon flux and reduce the undulator gain length. So, electron bunch length compression is critical for the flux of UV FEL photons interacting at the interaction point (IP). The return arc compressor in Fig. 1 gives a 205° beam deflection via a modified dou-

Content from this work may be used under the terms of the CC BY 3.0 licence (© 2019). Any distribution of this work must maintain attribution to the author(s), title of the work, publisher, and DOI

ble-bend achromatic cell magnetic structure characterized by a 3.58 Tm integrated bending field at $E=300$ MeV. The 6.5 m central arc trajectory length yields a bunch length compression factor $C \approx 15$ for 300 pC bunches, while limiting the growth of the transverse projected normalized emittances – here weakly affected by the emission of coherent synchrotron radiation (CSR) – to about $0.3 \mu\text{m}$.

The outgoing bunch has 0.5 kA peak current, $1 \mu\text{m}$ normalized projected emittances and $\sim 0.2\%$ correlated rms energy and energy distribution. Particle tracking indicates that CSR emission in the arc dipoles leads to some modulation in the bunch current profile FEL parameter threshold, and no relevant impact on the FEL performance is anticipated.

UV FEL

After bunch length compression the beam is injected into the undulator. In the 1-D approximation the FEL gain length is given in terms of the ‘FEL parameter’ ρ_{FEL} [12] by

$$L_G = \frac{\lambda_u}{4\pi\sqrt{3}\rho_{FEL}}. \quad (7)$$

The radiation bandwidth and the saturation power to electron beam power ratio scale linearly with the FEL parameter.

In the scenario depicted in Fig. 1 a helical undulator is proposed to maximize the output power of the UV FEL, reduce the gain length and provide transverse focusing. A compact design based on Permanent Magnet technology [8,18] can provide the desired field amplitude, such as $B_0=0.86$ T at $\lambda_u=20$ mm, and eventually an undulator parameter $a_u=1.60$. A ~ 5 m long undulator allows the FEL to reach saturation at the fundamental wavelength of 103 nm (12 eV photon energy). The analytical evaluation of the undulator length needed to reach saturation is shown in Fig. 3 as a function of the beam peak current, along with the final average gamma-ray photon flux. The FEL parameter is about 5.5×10^{-3} , the gain length 0.22 m and the FEL peak power at saturation 0.77 GW. The corresponding photon peak rate is 4×10^{26} UV ph/s.

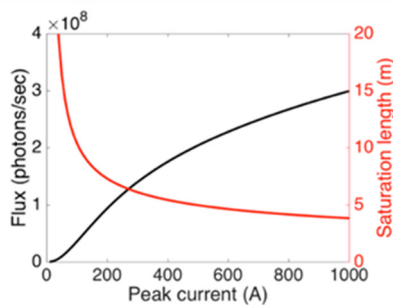


Figure 3: FEL-ICS performance in terms of scattered photon flux and FEL saturation length vs. the electron bunch peak current, for an undulator period length $\lambda_u=20$ mm.

Table 1: Electron beam parameters of the THz experimental sessions. (*) means “at the linac end”.

Parameter	Value	Units
Electron Beam Energy	300	MeV
Bunch Charge	300	pC
Bunch Duration, rms	2.5	ps
Bunch Peak Current	35	A
UV Photon Energy	12.0	eV
UV Peak Flux	2×10^{19}	photons/s
UV Duration, rms	0.16	ps
UV and e- rms beam sizes at IP (x / y)	60 / 15	μm
Interaction Angle	25	deg
Interacting e- Bunches per Train	90	
Interaction Rate	90	kHz
ICS Duty Factor	7.7×10^{-7}	
Scattered Photon Maximum Energy	~ 16	MeV
Scattered Photon Average Flux	1.1×10^8	photons/s mW
Scattered Photon Average Power	0.14	
Scattered Photon Average Intensity	1.8×10^7	photons/s/ mrad ²
Scattered Photon Peak Flux	1.4×10^{14}	photons/s mW
Scattered Photon Peak Power	1.8×10^5	
Scattered Photon Peak Intensity	2.3×10^{13}	photons/s/ mrad ²

CONCLUSIONS

By interacting with its own FEL radiation through an Inverse Compton Scattering process, a relatively low energy electron beam can simultaneously produce UV photons in the 10 to 12 eV range, and high-energy gamma-rays in the 6-16 MeV range. These photon beams can be used for Cultural Heritage, Nuclear Physics and UV science. A compact ~ 5 m long undulator is sufficient to simultaneously produce an UV flux of $\sim 2 \times 10^{19}$ ph/s and a high-energy photon flux in excess of 2×10^8 ph/s, within a system footprint of about 4×21 m². The scheme can be considered as an alternative to neutrons for the analysis of soil blocks of a certain volume containing archaeological findings like prehistoric teeth and old jewelry in the Geo-archaeology and Cultural Asset field. Moreover, it offers options for a wide range of multi-MeV photons applications in the Industry and Defense environments.

ACKNOWLEDGEMENT

Valuable contributions from G. D’Auria, L. Doolittle and F. Sannibale on Linac technical aspects are acknowledged and from D. Cocco for a feasibility estimate of a UV focusing system. This publication was funded by the Accelerators Group of Elettra Sincrotrone Trieste and by the Director, Office of Science, of the U.S. Department of Energy under Contract No. DE-AC02-05CH1123.

REFERENCES

- [1] M. Placidi *et al.*, NIM A 855 (2017) 55-60.
- [2] F. Casali *et al.*, “X-ray computed tomography for damage assessment of cultural heritage assets”, Protection of Historical Buildings, PROHITECH 09, Mazzolani (ed), 2009 Taylor & Francis Group, London, ISBN 978-0-415-55803-7.
- [3] C. P. J. Barty, “Nuclear photonics with laser-based gamma rays”, SPIE Opt. Optoelectron. Paper 8080B-30 (2011), doi:10.1117/2.1201110.003681.
- [4] D. Micieli *et al.*, PRST-AB 19, 093401 (2016).
- [5] A. Curatolo *et al.*, “Analytical description of photon beam phase spaces in Inverse Compton Scattering sources”, arXiv:1705.07740v1 [physics.acc-ph], 22 May 2017.
- [6] H. Motz, W. Thon and R.N. Whitehurst, “Experiments on Radiation by Fast Electron Beams”, J. Appl. Phys. **24**, No. 7, (1953) 826, doi:10.1063/1.1721389.
- [7] C. Pellegrini, A. Marinelli and S. Reiche, “The physics of free-electron lasers”, Reviews of Modern Physics **88** (2016) 015006, doi:10.1103/RevModPhys.88.015006.
- [8] A. B. Temnykh, “Delta undulator for Cornell energy recovery linac”, Phys. Rev. ST Accel. Beams **11** (2008) 120702, doi:10.1103/PhysRevSTAB.11.120702.
- [9] S. Sasaki, “Analyses for a planar variably-polarizing undulator”, Nucl. Instr. Meth. A **347** (1994) 83-86, doi:10.1016/0168-9002(94)91859-7.
- [10] S. Di Mitri and M. Cornacchia, “Transverse emittance-preserving arc compressor for high-brightness electron beam-based light sources and colliders”, EPL **109** (2015) 62002, doi:10.1209/0295-5075/109/62002.
- [11] S. Di Mitri, “Feasibility study of a periodic arc compressor in the presence of coherent synchrotron radiation” Nucl. Instr. Meth. A **806** (2015) 184-192, doi:10.1016/j.nima.2015.10.015.
- [12] R. Bonifacio, C. Pellegrini and L. M. Narducci, “Collective instabilities and high-gain regime in a free electron laser”, Opt. Commun. **50** (1984) 373, doi:10.1016/0030-4018(84)90105-6.
- [13] G. D’Auria, “Application of X-Band Linacs”, Proc. LINAC2012, Tel-Aviv, Israel (2012) 724-728, ISBN 978-3-95450-122-9.
- [14] C. Christou, “X-band linac technology for a high repetition rate light source”, Nucl. Instr. Meth. A **657** (2011) 13, doi:10.1016/j.nima.2011.06.050.
- [15] C. Limborg-Deprey *et al.*, “Achieved Performance of an All X-Band Photo-Injector”, Proc. IPAC2016, Busan, Korea. (2016) 4253, ISBN 978-3-95450-147-2.
- [16] R. Bartolini, “Beam dynamics optimisation of an X-band Linac driven soft X-ray FEL”, Nucl. Instr. Meth. A **657** (2011) 177, doi:10.1016/j.nima.2011.06.046.
- [17] C. Limborg-Deprey *et al.*, “Achieved Performance of an All X-Band Photo-Injector”, Proc. IPAC2016, Busan, Korea. (2016) 4253, ISBN 978-3-95450-147-2.
- [18] H.-D. Nuhn *et al.*, “Commissioning of the Delta Polarizing Undulator at LCLS”, Proc. FEL2015, Daejeon, Korea (2015) 757-763, ISBN 978-3-95450-134-2.